Inorganic Chemistry

Article

pubs.acs.org/IC

Uranyl-Peroxide Nanocapsules: Electronic Structure and Cation Complexation in $[(UO_2)_{20}(\mu\text{-}O_2)_{30}]^{20-}$

Pere Miro[†] and Carles Bo*[,†,‡]

[†]Institute of Chemical Research of Catalonia (ICIQ), 43007 Tarragona, Spain

[‡]Department de Química Física i Inorganica, Universitat Rovira i Virgili, 43007 Tarragona, Spain

Supporting Information

ABSTRACT: The pentagonal $K_{10}[(UO_2)_5(\mu\text{-}O_2)_5(C_2O_4)_5]$ species have been identified as the building blocks of uranyl-peroxide nanocapsules. The computed complexation energies of different alkali cations (Li^+, Na^+, K^+, Rb^+, and Cs^+) with $[(UO_2)_5(\mu\text{-}O_2)_5(O_2)_5]^{10-}$ and $[(UO_2)_{20}(\mu\text{-}O_2)_{30}]^{20-}$ species suggest a strong cation templating effect. In the studied species, the largest complexation energy occurs for the experimentally used alkali cations (Na^+ and K^+).

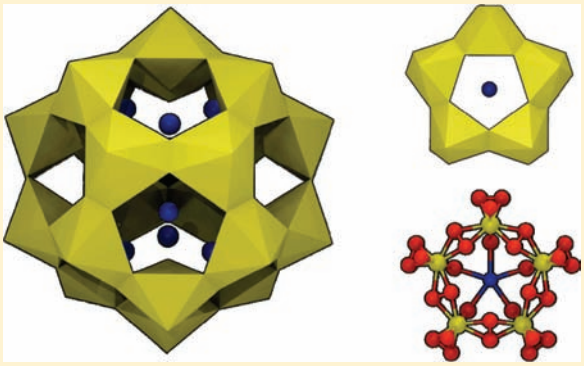

INTRODUCTION

Uranium is the second most abundant actinide in the Earth's crust and a fundamental energy source in our highly energy-demanding era. Thousands of tons of uranium ore are extracted every year from the earth's crust in the form of uraninite in Kazakhstan, Canada, and Australia.[1] The uranium ore can be directly used as a nuclear fuel in CANDU reactors, but usually a ^{235}U enrichment process is performed to generate the isotopically enriched uranium fuel usually used in one of the hundreds of nuclear power plants scattered around the globe. Large amounts of nuclear waste have been produced since the development of the first nuclear reactor. Many countries have stored their nuclear waste in temporary or permanent repositories; however, only a few, such as France or Pakistan, are reprocessing a considerable amount of nuclear waste through the highly complex and expensive plutonium and uranium recovery by extraction (PUREX) process.[2]

Understanding the solution chemistry of actinides, especially uranium and neptunium, is fundamental to developing an advanced nuclear energy cycle, including stored nuclear waste reprocessing. Toward the goal of developing new reprocessing techniques, Burns and co-workers synthesized a new family of uranyl-peroxide polyoxometalate nanocapsules obtained under favorable conditions in an alkaline peroxide environment.[3] In the past few years, numerous nanocapsules with up to 60 uranyl moieties have been reported presenting a wide variety of high symmetric topologies, including fullerene-like structures.[4,5] The self-assembly of uranyl small building blocks in aqueous solution under ambient conditions is unique in uranium chemistry, having a wide range of potential applications in fabrication and reprocessing of actinide-based materials.

In all cases, the uranyl ions are coordinated through six ligands arranged at the equatorial vertices of hexagonal bipyramids, the apexes of which correspond to the oxygen atoms of the uranyl dication. Each bipyramid binds to its neighbors through shared equatorial ligands. Since peroxide (μ-O_2) and hydroxide (μ-$OH)_2$ bridges are the most common, several types of square, pentagonal, and hexagonal faces are observed in the uranyl-peroxide nanocapsules, such as fully peroxide and mixed peroxide–hydroxide faces. Moreover, uranyl polyhedra nanocapsules, including other bridging ligands in their structure, such as pyrophosphate and oxalate, have been reported.[6−8] The critical influence of alkali cations present in solution during the nanocapsule synthesis has been demonstrated both experimentally[5−10] and theoretically.[11,12] The angle between the uranium centers and the peroxide moieties (U–O_2–U) is highly flexible and can adjust depending on the alkali cation present in the structure. Furthermore, it has been suggested that the alkali cations are the driving force for constructing the building blocks with geometries suitable to self-assemble into nanocapsules a posteriori.[11] However, the alkali cation's role in the growth of these species is not completely known since mechanistic studies are rare, and only very recently has the formation mechanism of the uranyl-peroxide dimer been proposed.[13]

Recently, our group studied the electronic structure of several cyclic uranyl-peroxide species (tetramers, pentamers, and hexamers) and their interaction with monovalent alkali cations using density functional theory (DFT)-based methods.[11] These species were identified as the fundamental

Received: January 5, 2012
Published: March 8, 2012

ACS Publications © 2012 American Chemical Society

dx.doi.org/10.1021/ic300029d | *Inorg. Chem.* 2012, 51, 3840–3845

building blocks that self-assemble a posteriori into uranyl-peroxide nanocapsules. Concurrently, Vlaisavljevich et al.[12] studied dimeric uranyl-peroxide species using the complete active space self-consistent field (CASSCF) calculations. Both studies conclude that the nature of the uranyl−peroxide bond is primarily ionic with an inherently bent bridging peroxide due to electronic effects. Nevertheless, these studies were focused on small building blocks, and to our knowledge, this is the first computational study on a complete uranyl-peroxide nanocapsule.

Here, we report studies on the smallest known uranyl-peroxide nanocapsule $[(U^{VI}O_2)_{20}(\mu\text{-}O_2)_{30}]^{20-}$ (U_{20}), which consists of 12 fused pentagonal faces forming a dodecahedron, and we compare it with the pentagonal $[(U^{VI}O_2)_5(\mu\text{-}O_2)_5(O_2)_5]^{10-}$ (U_5) species. U_5 is analogous to the building block experimentally isolated by Sigmon et al.[9] with peroxo ligands replacing the oxalate groups. Experimentally, both structures have cations under the pentagonal faces; consequently, we have studied the interaction between the U_5 and U_{20} species and alkali cations (Li^+, Na^+, K^+, Rb^+, and Cs^+) (Figure 1).

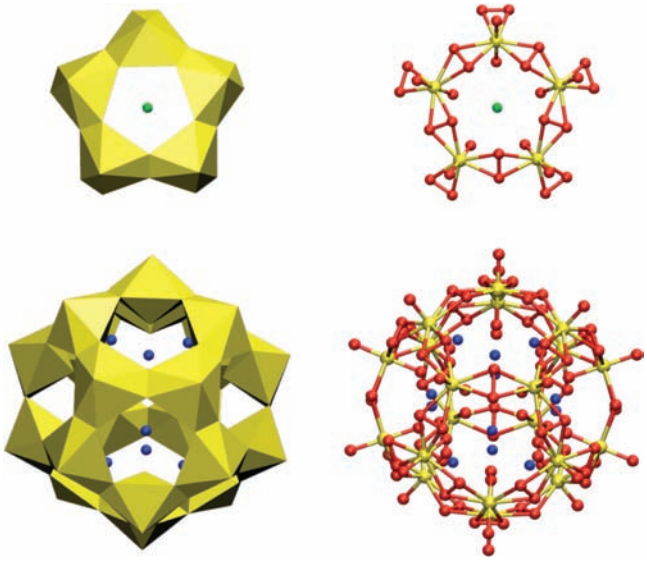

Figure 1. Polyhedral (top-left) and ball-and-stick (top-right) representations of the structure of the $K[(U^{VI}O_2)_5(\mu\text{-}O_2)_5(O_2)_5]^{9-}$ species. Polyhedral (bottom-left) and ball-and-stick (bottom-right) representations of the structure of the $Na_{12}[(U^{VI}O_2)_{20}(\mu\text{-}O_2)_{30}]^{8-}$ uranyl-peroxide nanocapsule. Uranium in yellow, oxygen in red, potassium in green, and sodium in blue.

COMPUTATIONAL DETAILS

All DFT calculations were performed using the Amsterdam Density Functional (ADF 2009) program developed by Baerends, Ziegler, and co-workers.[14] We used the local VWN exchange-correlation potential[15] with GGA Becke's exchange correction[16] and Perdew's correlation correction[17,18] (BP86). Relativistic corrections were introduced by scalar-relativistic zero-order regular approximation (ZORA).[19,20] A triple-ζ plus one polarization function basis set was used on all atoms. For non-hydrogen atoms, a relativistic frozen-core potential was used. Solvent effects were introduced by using the continuous solvent model COSMO[21] with Allinger[22] and Bragg[23] radii. The complexation energies were evaluated using alkali radii derived from Kelly et al.[24] (see the Supporting Information for details). Geometries were optimized under C_{5v} symmetry for U_5 (except U_5-Li, where C_s was used) and under D_{3d} symmetry for U_{20}. All U_5 structures were characterized by harmonic vibrational analysis.[25] Some structures presented low imaginary frequencies corresponding to orientation of the peroxide ligands outside the cycle due to the symmetry constraint. The dispersion energy of the cage was included a posteriori using the DFT-D3 package[26] developed by Prof. Grimme. Standard BP86 parameters with Becke and Johnson damping functions were used.[27−29]

RESULTS AND DISCUSSION

Uranyl-Peroxide Structures. In 2009, Sigmon et al.[9] synthesized the smallest known uranyl-peroxide nanocapsule, $Na_{20}[(U^{VI}O_2)_{20}(\mu\text{-}O_2)_{30}]$ containing 12 pentagonal faces. Furthermore, the X-ray diffraction structure reveals a Na^+ cation under each of the faces. The inner cavity is completely filled by the alkali cations, not leaving enough space to encapsulate other species inside as it occurs in larger nanocapsules.[30] Experimentally the addition of oxalate ligands during synthesis prevents the closure of nanocapsules, allowing the isolation of a pentagonal building block $K_{10}[(UO_2)(\mu\text{-}O_2)_5(C_2O_4)_5]$. The pentagonal building block U_5 possesses similar features to the nanocapsule faces: (i) all of the uranium atoms in each pentagon are in a plane, (ii) all U−(O_2)−U bridges have a butterfly bending of the peroxide oxygens ($O_{peroxide}$) connected to the uranium atoms, and (iii) oxo moieties in the uranyl ion (O_{uranyl}) are not aligned with the uranium center, but tilted, with one set of the oxygen atoms slightly pointing toward the center of the pentagon, maximizing its interaction with the alkali cation. This interaction leads to a shorter O_{uranyl}−O_{uranyl} distance where the tilting occurs. Thus, we studied a pentagonal building block with peroxo ligands $[(U^{VI}O_2)_5(\mu\text{-}O_2)_5(O_2)_5]^{10-}$ (U_5) and the complete $[(U^{VI}O_2)_{20}(\mu\text{-}O_2)_{30}]^{20-}$ (U_{20}) nanocapsule with 12 pentagonal units equivalent to the one present in the U_5 species.

We validated the structure of the U_5 building block by comparison with the available X-ray structure of the pentagonal building block, but also with the pentagonal faces present in U_{20}, U_{28}, and U_{60} nanocapsules.[3,9,10] All U_5 structures with and without a cation were optimized under C_{5v} symmetry with the cation sitting in the center of the ring and below the plane defined by the O_{uranyl} oxygen atoms. (Figure 1, top). The only exceptions are the structures with Li^+. Because of its small size, the cation is held in place by only three O_{uranyl} centers. Select experimental and computational geometric parameters are collected in Table 1. The computed distances are in very good agreement with experimental data, with only small discrepancies in almost all of the interatomic distances. However the O_{uranyl}−O_{uranyl} and O_{uranyl}−cation distances between the oxygen atoms of the uranyl moieties fluctuate significantly depending on whether or not a cation is in contact and on the cation's nature. Both distances and the dihedral are in better agreement with the X-ray structure when the experimental K^+ cation is included with an average deviation of 0.03 Å and 1.3°, respectively. Furthermore, these structures are in perfect agreement with the pentagonal faces present in uranyl-peroxide nanocapsules.

The cation complexation induces small structural changes into the U_5 structure since only the uranyl moieties are tilted toward the cation. In consequence, the U−O_2−U dihedral angle deviates. This moiety is always butterflied in the U_5 structures independent of the presence of a coordinated cation. All bonded interatomic distances, angles, and dihedrals show that U_5 reproduces the experimental building block isolated by

dx.doi.org/10.1021/ic300029d | Inorg. Chem. 2012, 51, 3840−3845

Table 1. Experimental (X-ray) and Computed (DFT) Geometrical Parameters of Interest (in Å and deg) of U_5-X and U_{20}-X_{12}

	DFT									experimental X-ray			
	U_5-X			U_{20}-X_{12}						U_5[a]	U_{20}[a]	U_{28}[b]	U_{60}[c]
	ø	Na^+	K^+	ø	Li^+	Na^+	K^+	Rb^+	Cs^+	K^+	Na^+	K^+	K^+
U−U	4.35	4.29	4.38	4.23	4.15	4.27	4.39	4.45	4.49	4.29	4.17	4.17	4.29
$U-O_{peroxide}$	2.40	2.41	2.41	2.40	2.35	2.38	2.41	2.44	2.46	2.39	2.33	2.37	2.39
$U-O_{uranyl}$	1.88	1.89	1.89	1.84	1.88	1.86	1.84	1.84	1.83	1.84	1.81	1.81	1.82
$O_{peroxide}-O_{peroxide}$	1.49	1.49	1.49	1.48	1.48	1.48	1.48	1.47	1.47	1.47	1.53	1.57	1.49
$O_{uranyl}-O_{uranyl}$[d]	3.34	3.00	3.28	2.95	2.79	2.93	3.07	3.14	3.19	3.30	2.83	3.04	3.28
O_{uranyl}−cation		2.56	2.85		2.41	2.55	2.76	2.87	2.96	2.81	2.39	2.74	2.83
$U-(O_{peroxide})_2-U$	144.4	138.9	145.7	134.2	137.3	142.1	146.1	146.5	146.7	144.4	139.0	141.8	144.6
Θ	28.4	49.1	25.2	31.7	31.7	31.7	31.7	31.6	31.7	≈18.2[e]	31.9		

[a]Reference 9. [b]Reference 3. [c]Reference 10. [d]Oxygens form two adjacent uranyls that host the cation. [e]Different Θ angles are present in the crystal structure due to crystal packing effects.

Sigmon et al;[9] however, this species does not include the nanocapsule structural constraints. We define Θ as the angle between the direction perpendicular to the uranium plane and the direction perpendicular to the $O_{peroxide}-O_{peroxide}$ bond as a parameter to account for the concavity of the faces (see Figure S6 in the Supporting Information). In the U_5 models, Θ is highly influenced by the presence of a cation in the center of the ring, being 49.1° and 25.2° in U_5-Na and U_5-K, respectively. This is in agreement with unconstrained peroxide ligands able to relax Θ to accommodate different alkali cations, which is impossible in the nanocapsules.

The experimental U_{20} nanocapsule contains 12 pentagonal faces sharing edges and a Na^+ alkali cation under each face. The relevant distances and angles of the optimized nanocapsule with and without alkali cations are presented in Table 1. Analogous to the U_5 species, the agreement between the calculated and the U_{20} X-ray structure is significantly improved when the 12 experimentally encapsulated Na^+ cations are included. In this case, the average distance and dihedral deviations in U_{20}-Na_{12} are just 0.09 Å and 3.1°, respectively. Moreover, regardless of the presence or absence of alkali cations, the $U-(O_2)-U$ moieties are always bent. The Θ angle in U_{20}-X_{12} species is constant, independent of the encapsulated cation, in contrast with its strong influence on U_5-X species. This is in perfect agreement with the structural constraints imposed by the spherical shape of the nanocapsules.

The nature of the encapsulated cation directly influences the geometry of the nanocapsule by causing the deformation of the cation-free capsule. The root-mean-square deviation (rmsd) is a similarity parameter of one structure with respect to a reference, zero for identical structures or a positive number if not. The rmsd induced by the presence of the alkali cations in the U_{20} nanocapsule are presented in Table 2 (see the Supporting Information for details). The monovalent alkali cations' size increases down the period ($Li^+ < Na^+ < K^+ < Rb^+ < Cs^+$); however, the radius of the cation is not correlated with the rmsd in the U_{20} nanocapsule. On one hand, the Li^+ cation is too small to be hosted by the O_{uranyl} moieties in the pentagonal units, and consequently, the capsule is deformed to maximize the cation$-O_{uranyl}$ interaction. Precisely, the uranyl moieties move toward the center of the nanocapsule to host the Li^+ cation. On the other hand, large cations, such as Rb^+ and Cs^+, require large deformations to be accommodated. In this case, the uranyl moieties are displaced away from the nanocapsule center (see Figure S7 in the Supporting Information). However, among the studied ions, Na^+ fits perfectly into the available space, inducing a minimum deformation with the largest cation$-O_{uranyl}$ interaction.

Table 2. Root-Mean-Square Deviations (rmsd) between Nanocapsules with Alkali Cations (U_{20}-X_{12}) and the Empty U_{20} Structure[a]

	root-mean-square deviation (rmsd)			deformation energy
alkali cation	U_{20}	peroxide O_2^{2-}	uranyl $(UO_2)^{2+}$	
Li^+	0.17	0.18	0.19	14.0
Na^+	0.08	0.10	0.07	36.1
K^+	0.14	0.01	0.13	10.0
Rb^+	0.21	0.07	0.20	72.5
Cs^+	0.26	0.13	0.26	119.3

[a]Total rmsd has been decomposed in uranyl and peroxide contributions. Cage deformation energies respect the cation-free U_{20} in solution. Energies per pentagonal unit (in kcal·mol^{-1}).

The rmsd can be split into contributions from the uranyl $(UO_2)^{2+}$ and peroxide $(O_2)^{2-}$ moieties, localizing the origin of the structural deformation. The Li^+ cation presents similar partial rmsd's in both moieties, in agreement with the small calculated $U-O_2-U$ dihedral induced by the approach of the uranyl group to host the Li^+. Large cations push the uranyl units out, but due to the flexibility of the $U-O_2-U$ bond, the peroxide moieties are almost unaltered. Both Na^+ and K^+ present the lowest average partial rmsd for uranyl and peroxide moieties.

We computed the cage deformation energy of each capsule with respect to the cation-free U_{20} since the rmsd is a similarity indicator, not an energy one (Table 2). Energetically, to incorporate K^+ into the U_{20} structure requires the lowest energy per pentagonal unit (10 kcal·mol^{-1}); meanwhile, larger cations, such as Rb^+ or Cs^+, require much more energy. The rsmd values indicate that Li^+ induces a larger deformation in the U_{20} cage than Na^+; however, energetically, the deformation induced by Li^+ cations requires less energy. One has to be aware that the deformation energies do not include the cation−capsule interaction or the cost to desolvate the free alkali cations to encapsulate them into the U_{20} structure. The complete cation complexation energies, including all these terms, are presented in the forthcoming section.

Electronic Structure. We studied the electronic structure of both U_5 and U_{20} species with and without cations through a frontier orbital analysis, as its utility in the study of uranyl-peroxide species has been previously demonstrated.[11,12] All studied species show a archetypical polyoxometalate electronic structure with empty f uranium orbitals composing the first set

dx.doi.org/10.1021/ic300029d | Inorg. Chem. 2012, 51, 3840−3845

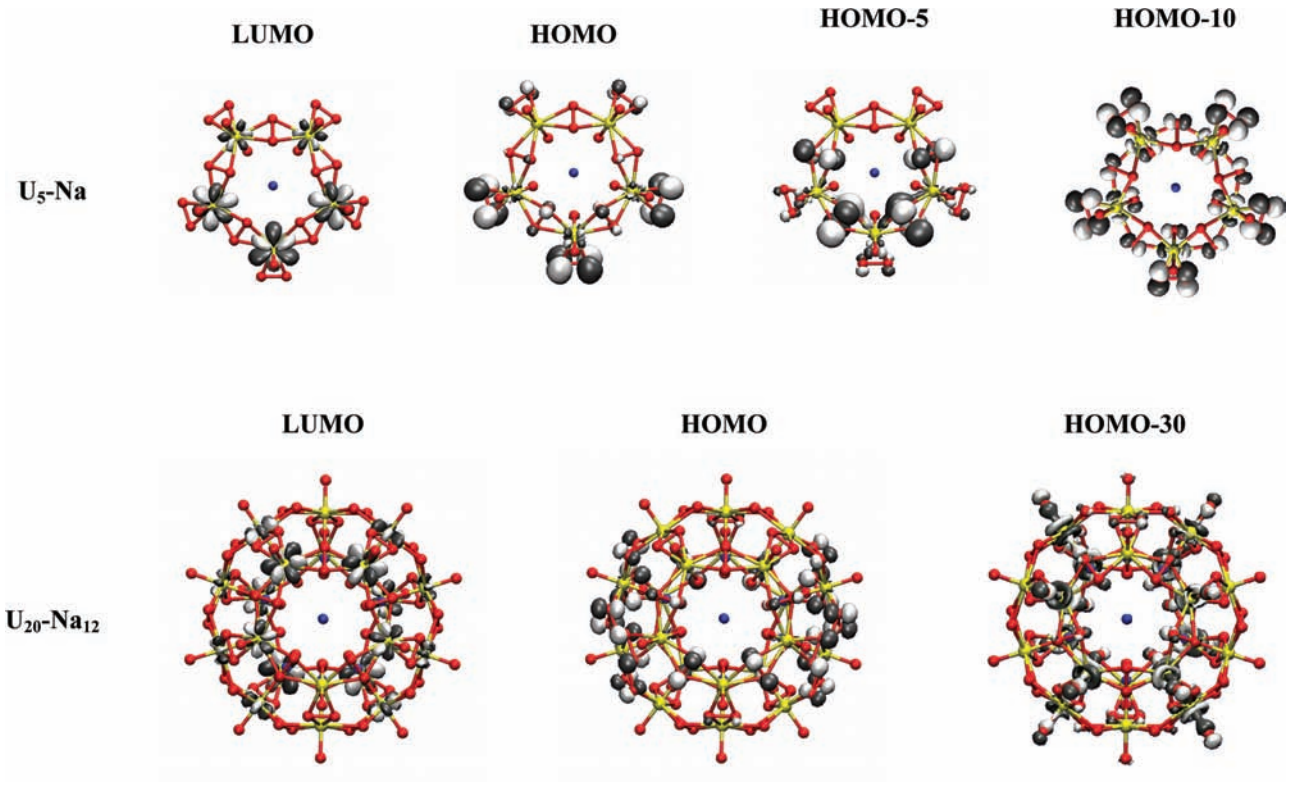

Figure 2. Relevant frontier orbitals for the U_5-Na species (top) and U_{20}-Na_{12} nanocapsule (bottom). Uranium in yellow, oxygen in red, and sodium in blue (isovalue = 0.03).

of empty energy levels (metal band), while the highest occupied orbitals belong to the oxo and peroxo moieties (oxo/peroxo band). This polyoxometalate nature allows us to clearly identify the peroxo band ranging from HOMO to HOMO-m−1, where m is the number of peroxide moieties. The oxo band lies right under the peroxo band and is completely dominated by the uranyl moiety orbitals. The frontier orbitals of U_5-Na and U_{20}-Na_{12} species are presented in Figure 2.

On one hand, the peroxo band in the U_5 species (HOMO to HOMO-4 and HOMO-5 to HOMO-9) is an antibonding combination of the peroxo π^* orbitals with a small bonding contribution from the uranium centers. On the other hand, this band (HOMO to HOMO-29) in the nanocapsule has no contributions from the uranium centers at all. Consequently, the peroxo−uranium bonding interaction on the pentagonal building block is a consequence of the lack of constraint and/or larger flexibility in comparison with the nanocapsule. The oxo bands located under the peroxo band are mainly the σ-bonding orbitals between the p oxo ligand and f uranium orbitals with some π-antibonding contribution of the peroxo bridge in both U_5-Na and U_{20}-Na_{12} species. The metal band is formed from empty f uranium orbitals in both species (LUMOs). The electronic structure of all the other species studied is analogous to the ones presented for U_5-Na and U_{20}-Na_{12}. As expected, alkali metal counterions do not contribute to the frontier energy levels.

Complexation Energy. In solution, ion complexation plays a fundamental role in a broad range of chemical phenomena, such as reactivity and redox properties, among others.[31−34] As mentioned above, the critical influence of alkali cations in the synthesis of uranyl-peroxide nanocapsules has been experimentally and computationally demonstrated. Table 3 displays

Table 3. Complexation Energies with and without Dispersion (in kcal·mol^{-1}) of the U_5-X and U_{20}-X_{12} Species with X = Li^+, Na^+, K^+, Rb^+, and Cs^+[a]

	U_5-X		U_{20}-X_{12}	
alkali	ΔE	ΔE + disp	ΔE	ΔE + disp
Li^+	−20.1	−29.6	−12.1	−26.0
Na^+	−22.0	−33.6	−20.3	−36.1
K^+	−22.9	−35.6	−18.9	−36.5
Rb^+	−20.1	−32.2	−11.1	−28.7
Cs^+	−18.8	−30.7	−5.7	−24.8

[a]Complexation energy per pentagonal unit.

the complexation energies induced by the ion complexation between the U_5 and U_{20} species and the monovalent alkali cations. Experimentally, only Na^+ and K^+ have been observed under pentagonal faces. Indeed, these cations stabilize the U_5 and the pentagonal units of U_{20} species the most, by 22.0 and 20.3 kcal·mol^{-1} for Na^+ and by 22.9 and 18.9 kcal·mol^{-1} for K^+, respectively. On one hand, smaller cations, such as Li^+, form weaker ion pairs due to the higher energy required to partially desolvate the cation. On the other hand, cations, such as Rb^+ and Cs^+, induce larger deformations to the nanocapsule and interact weakly due to their larger size, leading to smaller complexation energies of ca. 20 and 5−10 kcal·mol^{-1} for U_5-Rb/Cs and U_{20}-Rb_{12}/Cs_{12}, respectively. The addition of Grimme's DFT-D3 empirical dispersion energy corrections to the complexation energies always favors pairing without changing the observed trend, but increasing the diference between the complexation energies of Na^+/K^+ and the other alkali cations.[35]

These results reveal that the deformation energy presented in Table 2 is not the only term to take into account to describe

dx.doi.org/10.1021/ic300029d | Inorg. Chem. 2012, 51, 3840−3845

the ion complexation in uranyl-peroxide nanocapsules. The free alkali cation solvation/desolvation energy and obviously the electrostatic interaction between the uranyl-peroxide nanocapsule and the alkali cations also play a fundamental role. Consequently, Na^+ and/or K^+ seem the most suitable countercations for the stabilization of uranyl-peroxide nanocapsules containing pentagonal units

In uranyl-peroxide nanocapsules, the positions of the cations are usually determined through X-ray diffraction; however, this is not always possible due to crystal disorder. Fortunately, the electrostatic potential is directly related to the ion complexation positions. The molecular electrostatic potential of a "cation-free" U_{20} and U_{20}-Na_{12} nanocapsules are presented in Figure 3.

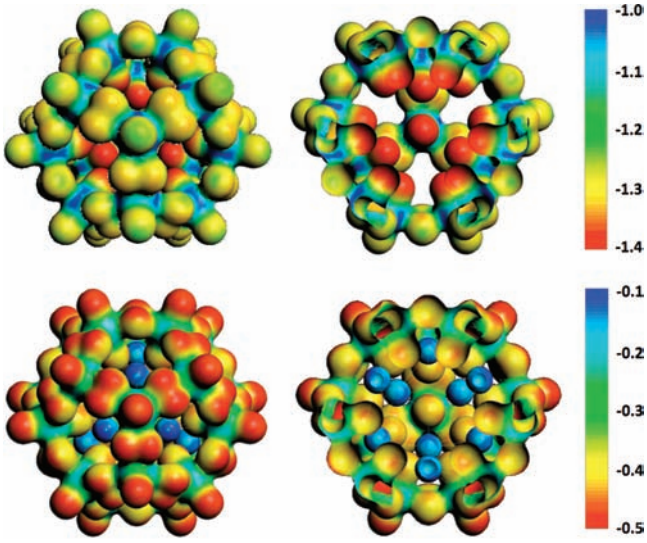

Figure 3. Molecular electrostatic potential mapped onto electron density isosurface of U_{20} (top) and U_{20}-Na_{12} (bottom) nanocapsules. On the right, a clipping plane was applied to enable viewing the internal cavity (isovalue = 0.03).

The U_{20} negative charge is spread among all the oxygen atoms; however, the internal O_{uranyl} hosts the most negative charge. This is in perfect agreement with the positions of the cations under the pentagonal faces observed experimentally. In U_{20}-Na_{12}, the capsule has reduced its charge through the complexation of 12 sodium cations. Consequently, the net charge on the oxygen centers are reduced, causing the external O_{uranyl} and $U_{peroxide}$ to become the most negatively charged. Recently, Nyman et al. reported the crystal structure of the U_{28} nanocapsule, in which large cations, such as Cs^+, lie on the external surface above the peroxide and between the external O_{uranyl}.[30] This is in agreement with our results where the negative charge lies on the exterior of the nanocapsule when the inner positions are fully occupied. The other studied species present similar molecular electrostatic potential distributions (Supporting Information).

CONCLUSIONS

In conclusion, we have studied the smallest known uranyl-peroxide nanocapsule $[(U^{VI}O_2)_{20}(\mu\text{-}O_2)_{30}]^{20-}$ (U_{20}), comparing it with the pentagonal $[(U^{VI}O_2)_5(\mu\text{-}O_2)_5(O_2)_5]^{10-}$ (U_5) building block. The calculated U_5 and U_{20} structures are in good agreement with the experimental X-ray structures, having the lowest errors when the experimental alkali cations are included. Our study reveals the importance of the structural constrains imposed by the nanocapsule.

The previously reported strong affinity between the uranyl-peroxide species with Na^+ and K^+ has been extended to U_5 and U_{20} species. The cation complexation energy can be divided in three separated terms: (i) the interaction between the U_5 and U_{20} species and the monovalent alkali cations, including the cation−cation repulsion for U_{20}-X_{12} species, (ii) the cation solvation/desolvation energy term, and (iii) the deformation of the uranyl-peroxide nanocapsule. We used a set of radii derived from Kelly et al.[24] that reproduce the solvation energy of the free monovalent alkali ions as accurate as possible, since this is fundamental for the accurate evaluation of the complexation energy. We have demonstrated that both Na^+ and K^+ have the largest complexation energy, and K^+ requires the smallest deformation energy among all the monovalent alkali cations.

We have done one step into the study of the electronic structure and ion complexation of complete uranyl-peroxide nanocapsules. Although many fundamental questions about uranyl-peroxide nanocapsules remain, such as the experimental preference of one isomer over thousands of possible structures. This points to a subjacent stabilization rule similar to the fullerene, but of a completely different nature. Further studies will be carried out in this direction.

ASSOCIATED CONTENT

Supporting Information

COSMO radii, optimized structures of all studied species, orbitals, and electrostatic potentials. This material is available free of charge via the Internet at http://pubs.acs.org.

AUTHOR INFORMATION

Corresponding Author

*E-mail: cbo@iciq.es.

Notes

The authors declare no competing financial interest.

ACKNOWLEDGMENTS

Research supported by the Spanish Ministerio de Economia y Competitividad (MINECO) through project CTQ2011-29054-C02-02, by the Generalitat de Catalunya (2009SGR-00462), and the ICIQ Foundation. P.M. thanks the Generalitat de Catalunya for a FI fellowship (2009FIC00026). We thank Prof. Christopher J. Cramer (University of Minnesota) for sharing his solvation expertise and extremely useful discussions.

REFERENCES

(1) Dahlkamp, F. J. *Uranium Ore Deposits*; Springer-Verlag: Berlin, 1993.

(2) Denniss, I. S.; Jeapes, A. P. *The Nuclear Fuel Cycle*; Oxford Science Publications: Oxford, U.K., 1996.

(3) Burns, P. C.; Kubatko, K. A.; Sigmon, G.; Fryer, B. J.; Gagnon, J. E.; Antonio, M. R.; Soderholm, L. *Angew. Chem., Int. Ed.* **2005**, *44*, 2135.

(4) Fowler, P. W.; Manolopoulos, D. E. *An Atlas of Fullerenes*; Oxford University Press: Oxford, U.K., 1995.

(5) Forbes, T. Z.; McAlpin, J. G.; Murphy, R.; Burns, P. C. *Angew. Chem., Int. Ed.* **2008**, *47*, 2824.

(6) Unruh, D. K.; Ling, J.; Qiu, J.; Pressprich, L.; Baranay, M.; Ward, M.; Burns, P. C. *Inorg. Chem.* **2011**, *50*, 5509.

(7) Ling, J.; Qiu, J.; Sigmon, G. E.; Ward, M.; Szymanowski, J. E. S.; Burns, P. C. *J. Am. Chem. Soc.* **2010**, *132*, 13395.

(8) Ling, J.; Wallace, C. M.; Szymanowski, J. E. S.; Burns, P. C. *Angew. Chem., Int. Ed.* **2010**, *49*, 7271.

(9) Sigmon, G. E.; Ling, J.; Unruh, D. K.; Moore-Shay, L.; Ward, M.; Weaver, B.; Burns, P. C. *J. Am. Chem. Soc.* **2009**, *131*, 16648.
(10) Sigmon, G. E.; Unruh, D. K.; Ling, J.; Weaver, B.; Ward, M.; Pressprich, L.; Simonetti, A.; Burns, P. C. *Angew. Chem., Int. Ed.* **2009**, *48*, 2737.
(11) Miro, P.; Pierrefixe, S.; Gicquel, M.; Gil, A.; Bo, C. *J. Am. Chem. Soc.* **2010**, *132*, 17787.
(12) Vlaisavljevich, B.; Gagliardi, L.; Burns, P. C. *J. Am. Chem. Soc.* **2010**, *132*, 14503.
(13) Vlaisavljevich, B.; Miró, P.; Cramer, C. J.; Gagliardi, L.; Burns, P. C. *Understanding the growth mechanism of small uranyl peroxide clusters: A density functional theory study*. Presented at the 241st ACS National Meeting, Anaheim, CA, March 27−31, 2011.
(14) Velde, G. T.; Bickelhaupt, F. M.; Baerends, E. J.; Guerra, C. F.; Van Gisbergen, S. J. A.; Snijders, J. G.; Ziegler, T. *J. Comput. Chem.* **2001**, *22*, 931.
(15) Vosko, S. H.; Wilk, L.; Nusair, M. *Can. J. Phys.* **1980**, *58*, 1200.
(16) Becke, A. D. *Phys. Rev. A* **1988**, *38*, 3098.
(17) Perdew, J. P. *Phys. Rev. B* **1986**, *34*, 7406.
(18) Perdew, J. P. *Phys. Rev. B* **1986**, *33*, 8822.
(19) van Lenthe, E.; Baerends, E. J.; Snijders, J. G. *J. Chem. Phys.* **1993**, *99*, 4597.
(20) van Lenthe, E.; Baerends, E. J.; Snijders, J. G. *J. Chem. Phys.* **1994**, *101*, 9783.
(21) Klamt, A. *J. Phys. Chem.* **1995**, *99*, 2224.
(22) Allinger, N. L.; Yuh, Y. H.; Lii, J. H. *J. Am. Chem. Soc.* **1989**, *111*, 8551.
(23) Bragg, W. L. *Philos. Mag.* **1920**, 169.
(24) Kelly, C. P.; Cramer, C. J.; Truhlar, D. G. *J. Phys. Chem. B* **2006**, *110*, 16066.
(25) Cramer, C. J. *Essentials of Computational Chemistry: Theories and Models*, 2nd ed.; John Wiley & Sons: Chichester, U.K., 2004.
(26) Grimme, S.; Antony, J.; Ehrlich, S.; Krieg, H. *J. Chem. Phys.* **2010**, *132*, 154104.
(27) Becke, A. D.; Johnson, E. R. *J. Chem. Phys.* **2005**, *123*, 154101.
(28) Johnson, E. R.; Becke, A. D. *J. Chem. Phys.* **2005**, *123*, 024101.
(29) Johnson, E. R.; Becke, A. D. *J. Chem. Phys.* **2006**, *124*, 174104.
(30) Nyman, M.; Rodriguez, M. A.; Alam, T. M. *Eur. J. Inorg. Chem.* **2011**, 2197.
(31) Chen, E. Y. X.; Marks, T. J. *Chem. Rev.* **2000**, *100*, 1391.
(32) Marcus, Y.; Hefter, G. *Chem. Rev.* **2006**, *106*, 4585.
(33) Macchioni, A. *Chem. Rev.* **2005**, *105*, 2039.
(34) Szwarc, M. *Ions and Ion Pairs in Organic Reactions*; Wiley-Interscience: New York, 1972; Vol. *1*.
(35) Grimme's DFT-D3 dispersion energy correction is a two-body interaction. Consequently, the correction in the cation complexation process is mainly due to the interactions between the alkali cations and the uranyl-peroxide nanocapsule.